

Summer 7-1-2019

## Plasticizer Interaction With the Heart: Chemicals Used in Plastic Medical Devices Can Interfere With Cardiac Electrophysiology.

Rafael Jaimes

Damon McCullough

Bryan Siegel

Luther Swift

Daniel McInerney

*See next page for additional authors*

Follow this and additional works at: [https://hsrc.himmelfarb.gwu.edu/smhs\\_peds\\_facpubs](https://hsrc.himmelfarb.gwu.edu/smhs_peds_facpubs)



Part of the [Pediatrics Commons](#)

---

### APA Citation

Jaimes, R., McCullough, D., Siegel, B., Swift, L., McInerney, D., Hiebert, J., Perez-Alday, E., Trenor, B., Sheng, J., Saiz, J., Tereshchenko, L., & Posnack, N. (2019). Plasticizer Interaction With the Heart: Chemicals Used in Plastic Medical Devices Can Interfere With Cardiac Electrophysiology.. *Circ Arrhythm Electrophysiol*, 12 (7). <http://dx.doi.org/10.1161/CIRCEP.119.007294>

This Journal Article is brought to you for free and open access by the Pediatrics at Health Sciences Research Commons. It has been accepted for inclusion in Pediatrics Faculty Publications by an authorized administrator of Health Sciences Research Commons. For more information, please contact [hsrc@gwu.edu](mailto:hsrc@gwu.edu).

---

**Authors**

Rafael Jaimes, Damon McCullough, Bryan Siegel, Luther Swift, Daniel McInerney, James Hiebert, Erick A Perez-Alday, Beatriz Trenor, Jiansong Sheng, Javier Saiz, Larisa G Tereshchenko, and Nikki Gillum Posnack

ORIGINAL ARTICLE



# Plasticizer Interaction With the Heart

## Chemicals Used in Plastic Medical Devices Can Interfere With Cardiac Electrophysiology

See Editorial by Reilly et al

**BACKGROUND:** Phthalates are used as plasticizers in the manufacturing of flexible, plastic medical products. Patients can be subjected to high phthalate exposure through contact with plastic medical devices. We aimed to investigate the cardiac safety and biocompatibility of mono-2-ethylhexyl phthalate (MEHP), a phthalate with documented exposure in intensive care patients.

**METHODS:** Optical mapping of transmembrane voltage and pacing studies were performed on isolated, Langendorff-perfused rat hearts to assess cardiac electrophysiology after MEHP exposure compared with controls. MEHP dose was chosen based on reported blood concentrations after an exchange transfusion procedure.

**RESULTS:** Thirty-minute exposure to MEHP increased the atrioventricular node (147 versus 107 ms) and ventricular (117 versus 77.5 ms) effective refractory periods, compared with controls. Optical mapping revealed prolonged action potential duration at slower pacing cycle lengths, akin to reverse use dependence. The plateau phase of the action potential duration restitution curve steepened and became monophasic in MEHP-exposed hearts (0.18 versus 0.06 slope). Action potential duration lengthening occurred during late-phase repolarization resulting in triangulation (70.3 versus 56.6 ms). MEHP exposure also slowed epicardial conduction velocity (35 versus 60 cm/s), which may be partly explained by inhibition of  $\text{Na}_v1.5$  (874 and 231  $\mu\text{mol/L}$  half-maximal inhibitory concentration, fast and late sodium current).

**CONCLUSIONS:** This study highlights the impact of acute MEHP exposure, using a clinically relevant dose, on cardiac electrophysiology in the intact heart. Heightened clinical exposure to plasticized medical products may have cardiac safety implications—given that action potential triangulation and electrical restitution modifications are a risk factor for early after depolarizations and cardiac arrhythmias.

**VISUAL OVERVIEW:** A [visual overview](#) is available for this article.

Rafael Jaimes III, PhD  
Damon McCullough, BS\*  
Bryan Siegel, MD\*  
Luther Swift, PhD  
Daniel McInerney, BS  
James Hiebert, BS  
Erick A. Perez-Alday, PhD  
Beatriz Trenor, PhD  
Jiansong Sheng, PhD  
Javier Saiz, PhD  
Larisa G Tereshchenko,  
MD, PhD  
Nikki Gillum Posnack, PhD

\*D. McCullough and Dr Siegel contributed equally to this work

**Key Words:** action potentials  
■ electrophysiology ■ heart  
■ plasticizer ■ plastics

© 2019 The Authors. *Circulation: Arrhythmia and Electrophysiology* is published on behalf of the American Heart Association, Inc., by Wolters Kluwer Health, Inc. This is an open access article under the terms of the [Creative Commons Attribution Non-Commercial-NoDerivs](#) License, which permits use, distribution, and reproduction in any medium, provided that the original work is properly cited, the use is noncommercial, and no modifications or adaptations are made.

<https://www.ahajournals.org/journal/circep>



### WHAT IS KNOWN?

- Phthalate chemical exposure has been reported in patients undergoing invasive medical procedures that use large quantities of plastic materials.
- We previously reported that phthalate chemical exposure impairs cell coupling and slows conduction velocity in a cardiomyocyte cell model.

### WHAT THE STUDY ADDS?

- Acute phthalate exposure slowed atrioventricular conduction and increased atrioventricular node effective refractory period in an intact, whole heart model.
- Phthalate exposure prolonged action potential duration time, enhanced action potential triangulation, and increased the ventricular effective refractory period.
- Phthalate exposure slowed epicardial conduction velocity, which may be partly explained by inhibition of Nav1.5.

Plastics have revolutionized clinical care. Yet, despite the many advantages, concerns have been raised about the ubiquitous use of plastics in the clinical setting.<sup>1–3</sup> To manufacture flexible plastic products, phthalate esters are added to impart flexibility to otherwise stiff polyvinyl chloride polymers. Di-2-ethylhexyl phthalate (DEHP) is the most commonly used plasticizer in Food and Drug Association–approved medical devices, including blood storage bags, tubing circuits, enteral feeding tubes, endotracheal tubes, and catheters.<sup>4</sup> In the finished product, DEHP can contribute up to 40% by weight in intravenous bags and 80% by weight in medical tubing. Because phthalate esters are hydrophobic and noncovalently bound to the polyvinyl chloride polymer, these additives are highly susceptible to leaching when in contact with blood, plasma, and other lipophilic solutions.<sup>5,6</sup> Consequently, heightened phthalate exposure has been observed in patients undergoing invasive medical procedures that use large quantities of plastic materials—including cardiopulmonary bypass, extracorporeal membrane oxygenation, dialysis, and transfusion procedures (see Table).<sup>7–21</sup> As an example, a neonatal exchange transfusion procedure resulted in plasma concentrations as high as 38  $\mu\text{M}$  DEHP and 54  $\mu\text{M}$  mono-2-ethylhexyl phthalate (MEHP), the primary metabolite of DEHP.<sup>13</sup> Whereas multiple medical procedures can increase a patient's cumulative phthalate exposure to levels that are 4000 $\times$  to 160 000 $\times$  higher than deemed safe.<sup>7</sup> Importantly, phthalate levels can remain elevated in the blood for hours (eg, blood transfusion; 5–24 hour half-lives)<sup>22,23</sup> to weeks (eg, extracorporeal membrane oxygenation support, intensive care unit patient) depending on the course of treatment.<sup>19</sup>

Incidental plastic chemical exposure during medical procedures is virtually unavoidable, yet the direct impact on patient health remains unclear. Because phthalates structurally resemble natural hormones, they can exert endocrine-disrupting properties and interfere with an array of biological processes.<sup>7,24,25</sup> Moreover, these low molecular weight chemicals have been shown to interact with ion channels, nuclear receptors, and other cellular targets. Accordingly, phthalates are likely to have a global impact on human health that is multifactorial. Indeed, epidemiological studies have reported associations between phthalate exposure and a broad range of health conditions, including metabolic disturbances, reproductive disorders, inflammatory conditions, neurological disorders, and cardiovascular disease.<sup>24–31</sup> The latter is particularly worrisome—since patients who are most susceptible to hospital-based phthalate exposures are often at heightened risk for cardiovascular complications, including those undergoing multiple transfusions, chronic transfusions (sickle cell, thalassemia) or support procedures (extracorporeal membrane oxygenation, cardiopulmonary bypass, dialysis).<sup>4,9,19,32–34</sup> Local and systemic reactions to plastic chemicals may add an extra insult to patients who are prone to secondary complications, including hypoxia (congenital heart defect patients), ischemia-reperfusion injury (cardiac surgery patients), postoperative arrhythmias, cardiac iron overload, pulmonary hypertension, impaired contractility, and diastolic dysfunction.

Indeed, animal studies have shown a causal relationship between phthalate exposure and subsequent alterations in cardiovascular function.<sup>35–39</sup> Using a rodent heart-lung preparation, Labow, et al<sup>38</sup> showed that phthalates exert a hypertensive effect on the pulmonary vasculature. This group also showed that phthalate exposure has a negative inotropic effect on isolated human atrial trabeculae, thus highlighting the applicability to humans.<sup>36</sup> Our group has also shown that phthalate exposure alters calcium handling and contractility *in vitro*, using rodent and human cardiomyocytes.<sup>40,41</sup> Moreover, phthalate exposure was shown to reduce gap junctional connexin-43,<sup>40,41</sup> which decreased intercellular coupling and slowed conduction velocity (CV). Therefore, we hypothesized that phthalate exposure may directly impact cardiac electrophysiology in an intact heart.

To test this hypothesis, we comprehensively assessed the electrophysiological effects of MEHP using isolated, intact rodent hearts. Cardiac electrophysiology parameters were measured at baseline and again after treatment with either control or MEHP-supplemented media perfusion (30 minutes). To address clinical relevance, the MEHP dose (60  $\mu\text{M}$ ) selected for heart perfusion was comparable to patient exposure after an exchange transfusion procedure<sup>13</sup> or measured levels in stored blood products.<sup>4,42</sup>

**Table. Measurements of Clinical Exposure to DEHP and Its Metabolites Including MEHP**

Description	Concentration	Reference
Child, blood products (blood)	6.4–29 µg/mL DEHP (RBC unit)	Mallow et al <sup>7</sup>
	27.6–405 µg/mL DEHP (plasma unit)	
	34.2–61.4 µg/mL DEHP (platelets)	
Child, exchange transfusion (blood)	1.1–15.6 µg/mL MEHP	Sjöberg et al 1985 <sup>8</sup>
	2.3–19.9 µg/mL DEHP	
Child, blood products (blood)	3.0–15.6 µg/mL MEHP (blood unit)	Sjöberg et al 1985 <sup>13</sup>
	36.8–84.9 µg/mL DEHP (blood unit)	
Child, ECMO (blood)	26.8 µg/mL DEHP (14 days)	Shneider et al <sup>14</sup>
	33.5 µg/mL DEHP (24 days)	
Child, ECMO (blood)	10–30.8 µg/mL DEHP (circuit)	Karle et al <sup>15</sup>
	0–24.18 µg/mL DEHP (patient)	
Child, blood products (blood)	4.3–123 µg/mL DEHP (blood unit)	Plonait et al <sup>16</sup>
	6–21.6 µg/mL DEHP (patient)	
Child, intensive care unit (urine)	577–2357 µg/L MECPP	Gaynor et al <sup>17</sup>
	120–438 µg/L MEHHP	
	72–306 µg/L MEOHP	
	14.9–49.5 µg/L MEHP	
Child, intensive care unit (urine)	6.2–704 ng/mL MEHP (5th%–95th%)	Calafat et al <sup>18</sup>
	290–13 161 ng/mL MEHHP (5th%–95th%)	
	243–10 413 ng/mL MEOHP (5th%–95th%)	
Child, intensive care unit (urine)	0–1234 ng/mL MEHP	Demirel et al <sup>19</sup>
	0–5841 ng/mL MEOHP	
	0–5086 ng/mL MEHHP	
Child, intensive care unit (urine)	0.049–1.273 µg/mL	Su et al <sup>20</sup>
Adult, blood products (blood)	1.1–18.7 µg/mL MEHP	Peck et al <sup>10</sup>
	72.5–295.2 µg/mL DEHP	
Adult, intensive care unit (blood)	0–171 µg/L MECPP	Huygh et al <sup>21</sup>
	0–55.4 µg/L MEHHP	
	0–22.9 µg/L MEOHP	
Adult, ECMO + CVVH (blood)	17.2–5194 µg/L MECPP	Huygh et al <sup>21</sup>
	0–880 µg/L MEHHP	
	3.3–305 µg/L MEOHP	
Adult, coronary bypass (blood)	15.4–72.9 mg/d DEHP	Barry et al <sup>9</sup>
	2.2–8 mg/kg MEHP	
Adult, heart transplantation (blood)	2.3–167.9 mg/d DEHP	Barry et al <sup>9</sup>
	0.25–18.8 mg/d MEHP	
Adult, hemodialysis (blood)	0.3–7.6 µg/mL DEHP	Pollack et al <sup>11</sup>
	0.9–2.83 µg/mL MEHP	
Adult, hemodialysis (blood)	2–3 µg/mL DEHP	Faouzi et al <sup>12</sup>

CVVH indicates continuous venovenous hemofiltration; DEHP, di-2-ethylhexyl phthalate; ECMO, extracorporeal membrane oxygenation; MECPP, mono-2-ethyl-5-carboxypentyl phthalate; MEHHP, mono-2-ethyl-5-hydroxyhexyl phthalate; MEHP, mono-2-ethylhexyl phthalate; MEOHP, mono-2-ethyl-5-oxohexyl phthalate; and RBC red blood cell.

## METHODS

The authors declare that data that supports the findings of this study are available within the article.

### Isolated Heart Preparation

Animal protocols were approved by the Institutional Animal Care and Use Committee of the Children's Research Institute and followed the National Institutes of Health's *Guide for the Care and Use of Laboratory Animals*. Experiments were conducted using adult, male Sprague-Dawley rats (>8 weeks old, >280 g, Taconic Biosciences). Animals were housed in conventional rat cages in the Research Animal Facility under standard environmental conditions (12:12 hour light:dark cycle, 64°C–78°C, 30%–70% humidity, free access to reverse osmosis water, corn cob bedding, and food [2918 rodent chow; Envigo]). Animals were anesthetized with 3% to 5% isoflurane; the heart was excised and then transferred to a temperature-controlled (37°C) constant-pressure (70 mm Hg) Langendorff perfusion system for electrophysiology and optical mapping experiments. Excised hearts were perfused with Krebs-Henseleit buffer bubbled with carbogen throughout the duration of the experiment, as previously described (≈1 hour).<sup>43</sup>

### General Protocol

MEHP (93+%; Wako Chemicals) stock solution was prepared in 99+% dimethyl sulfoxide (DMSO), and the working concentration was prepared directly in perfusate media with a total DMSO concentration of <0.001%. To avoid bolus exposure, the perfusion system was designed to premix MEHP with perfusate media to the desired concentration before entering the aorta. Cardiac electrophysiology was assessed under baseline conditions (control media perfusion) and again after either control media perfusion or 60 µM MEHP-supplemented media perfusion (30 minutes). This allowed us to control for electrophysiology changes that could be attributed to procedure (control baseline versus control 30 minutes), individual animal differences, and MEHP treatment (control 30 minutes versus MEHP 30 minutes). For clinical relevance, the MEHP dose (60 µM) was selected based on an upper clinically relevant exposure after an exchange transfusion procedure<sup>13</sup> and within the range of measured levels in stored blood products.<sup>4,42</sup>

### Electrophysiology Measurements

A reference electrode was positioned proximal to the right atrium and a measuring electrode proximal to the apex to acquire a pseudo-ECG in the lead II configuration (differential amplifier with 1000× gain). During sinus rhythm, ECG signals were collected to analyze heart rate, beat rate variability, atrioventricular conduction (PR interval) depolarization time, and repolarization time ( $RJ_{point} RT$ ).<sup>44</sup> Signals were acquired in iox2 (emka Technologies), and ECG segments were computed in ecgAUTO (emka Technologies).

For determination of atrioventricular nodal effective refractive period (AVNERP), Wenckebach cycle length (WBCL), and sinus node recovery time, a coaxial stimulation electrode (Harvard Apparatus, Holliston, MA) was placed on the right

atrium. AVNERP was defined as the maximum extrastimulus interval (S1-S2) during atrial pacing that failed to conduct through the atrioventricular node, as indicated by loss of ventricular capture. WBCL was defined as the maximum pacing cycle length (PCL) during atrial pacing that caused the Wenckebach phenomenon. Sinus node recovery time was measured to assess the automaticity of the sinoatrial node and defined as the time delay between the last paced atrial depolarization and the first sinus beat (5 s electrical stimulation at 200 ms PCL). A stimulator (Bloom Electrophysiology, Denver, CO) was set to 1 ms pulse width at 1.5× diastolic current threshold. For ventricular pacing, a 0.25 mm diameter tungsten, unipolar, cathodal electrode was placed on the LV epicardium and centered in the imaging field. A stainless steel indifferent electrode was placed under the heart. To determine the ventricular effective refractory period (VERP) within 10 ms, dynamic pacing (S1-S1) was performed during optical mapping. An arrhythmia score was designated for each individual heart after the dynamic pacing protocol, wherein the most severe electrical disturbance was classified (1=single premature ventricular contraction [polyvinyl chloride], 2=bigeminy/salvos, 3=ventricular tachycardia or fibrillation).<sup>45</sup>

### Ventricular Conduction Frequency Composition Assessment

High resolution (2000 Hz) unfiltered digital pseudo-ECG recordings were analyzed using a custom MATLAB (MathWorks, Inc, Natick, MA) software application. Normal sinus median beat was constructed out of 436 normal sinus beats, as previously described.<sup>46</sup> Appropriate selection of beats was confirmed by investigator (Dr Perez-Alday) with the aid of a graphical display. From the median beat obtained, QRS was measured from QRS onset to J point.<sup>47</sup> The power spectral density (PSD) was measured on the median beat of the ECG signal<sup>48</sup> using a nonparametric Fast-Fourier transform algorithm based on the Welch-Bartlett power estimation method,<sup>49</sup> with a Hanning window of length 8 samples and a 50% overlap between segments. From the Nyquist frequency, the available frequency range was from 0 to 1000 Hz; however, the frequency composition was calculated on 5 subsets of 100 Hz frequency intervals from 0 Hz to 500 Hz. The relative contribution of frequencies was normalized over the total power.

### Optical Mapping

After establishing a baseline heart rate (10 minutes), the perfusate was supplemented with 10  $\mu\text{mol/L}$  (–)-blebbistatin (Sigma-Aldrich) to reduce motion artifact for imaging experiments.<sup>50</sup> The heart was loaded with a potentiometric dye (62.1  $\mu\text{g}$  RH237, 1-minute staining) through a bubble trap located proximal to the aortic cannula.<sup>51,52</sup> The epicardium was illuminated with 2 broad light-emitting diode spotlights (530 nm, 200 mW; Mightex). RH237 fluorescence was longpass filtered (680+ nm; Chroma Technologies), and optical action potentials were acquired using a fixed focal lens (17 mm, f/0.95; Schneider Optics) attached to an sCMOS camera (Zyla 4.2 PLUS; Andor Technology). The camera sensor was cropped to 384×256 pixels and set to an exposure time of 1.219 ms resulting in the acquisition of 16-bit monochrome images at 814 frames per

second for 2 s. Optical maps were acquired during each PCL (S1-S1; 250–80 ms, 10 ms increments). A custom MATLAB (MathWorks, Natick, MA) script was used to calculate the action potential durations (APD) to percent repolarization (APD30, 80, 90) for every beat in the recording, as previously described. APD triangulation was defined as the difference between APD90 and APD30.<sup>53</sup> Restitution curves were generated by plotting APD80 against PCL; curves were then analyzed as either monophasic or biphasic (where applicable) to determine slopes, as indicated by Franz.<sup>54</sup> APD alternans were defined as sequential APD80 measurements that differed by >4 ms.

### Image and Signal Processing

Data analysis was performed using a custom MATLAB script. A region of interest (<20 pixel radius) was selected from the raw image, averaged, and plotted against time. Drift removal was performed by subtraction of a polynomial fit if necessary. To remove high-frequency noise, a fifth order Butterworth low-pass filter was applied to the resulting signals with a cutoff frequency adjusted between 50 and 150 Hz. A peak detector was then used to measure the total number of action potentials in the file across time. Characteristics from each event are measured and averaged, including APD30, APD80, and APD90, as described previously. Image processing was performed, and isochrone activation maps were constructed in RHYTHM.<sup>55</sup> The background was removed, convolved with a 15×15 uniform kernel for box blurring and then time signals were low-pass filtered below 100 Hz. The activation time of every pixel on the heart was defined as the maximum derivative of the action potential or transient upstroke. To measure epicardial CV, activation maps were subsequently loaded into ORCA<sup>56</sup> and measured at a minimum of 18 angles separated by 10° each from the pacing stimulus with the median CV reported. Subsequent electrical wave propagation images were then constructed using custom Python scripts and plotted with matplotlib.<sup>57</sup>

### Whole-Cell Voltage-Clamp Recordings

Recordings were performed at room temperature (22°C–25°C) using HEK293 (human embryonic kidney 293) cells stably transfected with Nav1.5 cDNA. For Nav1.5 recordings, the extracellular solution (mM) included 137 NaCl, 10 HEPES, 4 KCl, 1 MgCl<sub>2</sub>, 1 CaCl<sub>2</sub>, 10 dextrose, and the intracellular solution included 120 aspartic acid, 120 CsOH, 10 CsCl, 10 HEPES, 10 EGTA, 5 MgATP, 0.4 TrisGTP. The voltage protocol (1 s duration) was repeated at 0.1 Hz. Briefly, cells were repolarized from –95 to –120 mV for 200 ms, then depolarized from –120 to –15 mV for 40 ms, and further depolarized to +40 mV for 200 ms, followed by a voltage ramp down phase for 100 ms from +40 to –95 mV. Nav1.5 late current was induced by 20 nmol/L anemone toxin in the extracellular solution, which allowed for the study of late sodium current contribution from Nav1.5 that is separate from fast sodium current, as previously described.<sup>58</sup> Nav1.5 fast current was measured in the absence of anemone toxin. For positive control, 30  $\mu\text{M}$  tetrodotoxin (sodium channel blocker) was directly applied to recordings and resulted in 98.3±0.7% Nav1.5 current block (n=3). To ensure baseline recording was stable enough for drug application, cells were presented with this voltage



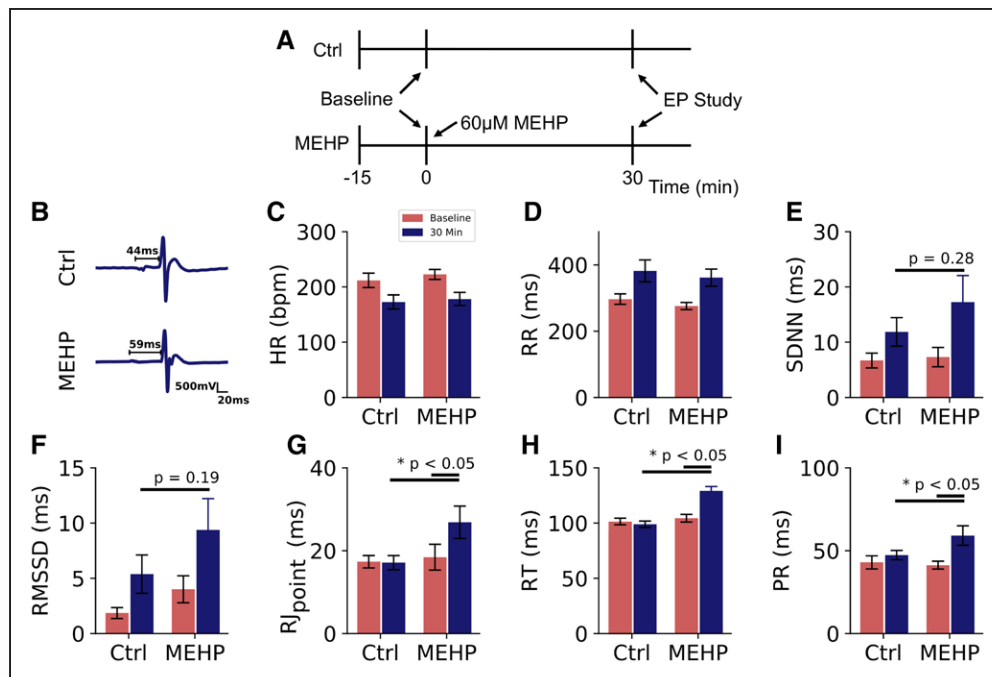


**Figure 1.** Effect of mono-2-ethylhexyl phthalate (MEHP) on ECG characteristics during sinus rhythm.

**A**, Experimental protocol timeline; all ECG recordings were performed during sinus rhythm. **B**, ECG signals collected from excised, intact rat hearts with PR interval denoted. **C**, Heart rate (HR) decreased with time of perfusion and after application of blebbistatin for mechanical uncoupling, with no difference between treatment groups. **D**, Similar rate slowing was observed in the RR interval, and coincided with heart rate variability changes in **E** SD of the normal RR intervals (SDNN) and **F** root means successive square difference (rMSSD) after 30-min perfusion. **G** and **H**, Prolonged depolarization and repolarization in MEHP-exposed hearts as measured from R to J inflection point (RJ<sub>point</sub>) and R to T-wave (RT) (**G**) PR interval time was significantly lengthened in MEHP-exposed hearts compared to both baseline and control (Ctrl) hearts after the same duration of perfusion ( $P < 0.05$ ).  $n \geq 7$  per group. BPM indicates beats per minute; and EP, electrophysiology protocol.

protocol in control solution until Nav1.5 current amplitudes for 12 consecutively recorded current traces (2-minute duration) exhibit <10% difference. Effects were monitored for 3 minutes before and after application of MEHP ( $n = 4$  per dose). To quantify drug potency against Nav1.5 channels, the steady state Nav1.5 current amplitude (averaged value from 5 steady state current traces) in drug solution was divided by the averaged amplitude from the last 5 traces measured in control solution to calculate the fractional block. Then, fractional block was plotted against drug concentration tested, fitted with the Hill Equation to generate an half-maximal inhibitory concentration (IC<sub>50</sub>) and the Hill coefficient.

### In Silico Modeling

Human ventricular action potentials were simulated using previously established models and conductance.<sup>59,60</sup> The block of fast and late sodium,  $I_{Na}$  and  $I_{NaL}$ , respectively, were provoked with the computed IC<sub>50</sub> from MEHP determined by whole-cell recordings (see previous section) as previously described.<sup>62</sup> The isolated epicardial cellular model was paced with 1000 pulses ( $-80 \mu A/\mu F$ , 0.5 ms) at PCL=250 ms in the presence of 60  $\mu mol/L$  MEHP.

### Statistical Analysis

Statistical analysis was performed using the R software package and Stata MP 15.1 (StataCorp, College Station, TX). Data normality was confirmed by Shapiro-Wilk test. Datasets were compared using a 2-sample Student independent *t* test

between the 2 treatment groups (30-minute control, 30-minute MEHP treated) or paired *t* test between baseline and 30-minute time points. Significance was defined as  $P \leq 0.05$ . Results were reported as mean  $\pm$  SE mean, from a minimum of 5 animals per group as indicated. As distribution of PSD variables was skewed, we used Wilcoxon rank-sum test to compare groups (control versus MEHP treated). Wilcoxon matched-pairs signed-ranks test was used for paired comparison of PSD changes before and after MEHP treatment. Variables with skewed distribution are presented as median and interquartile range. Arrhythmia incidence was compared using the  $\chi^2$  test.

## RESULTS

### Effects of MEHP Exposure on Cardiac Automaticity and Beat Rate Variability During Sinus Rhythm

ECG characteristics were quantified at 2 time points—first under baseline conditions and again after 30 minutes of control or 60  $\mu M$  MEHP-supplemented media perfusion during sinus rhythm (Figure 1A). Example ECG traces are shown in Figure 1B. Heart rate at 30 minutes was comparable between experimental groups, 172 beats per minute in control and 178 beats per minute in MEHP-treated hearts (Fig-

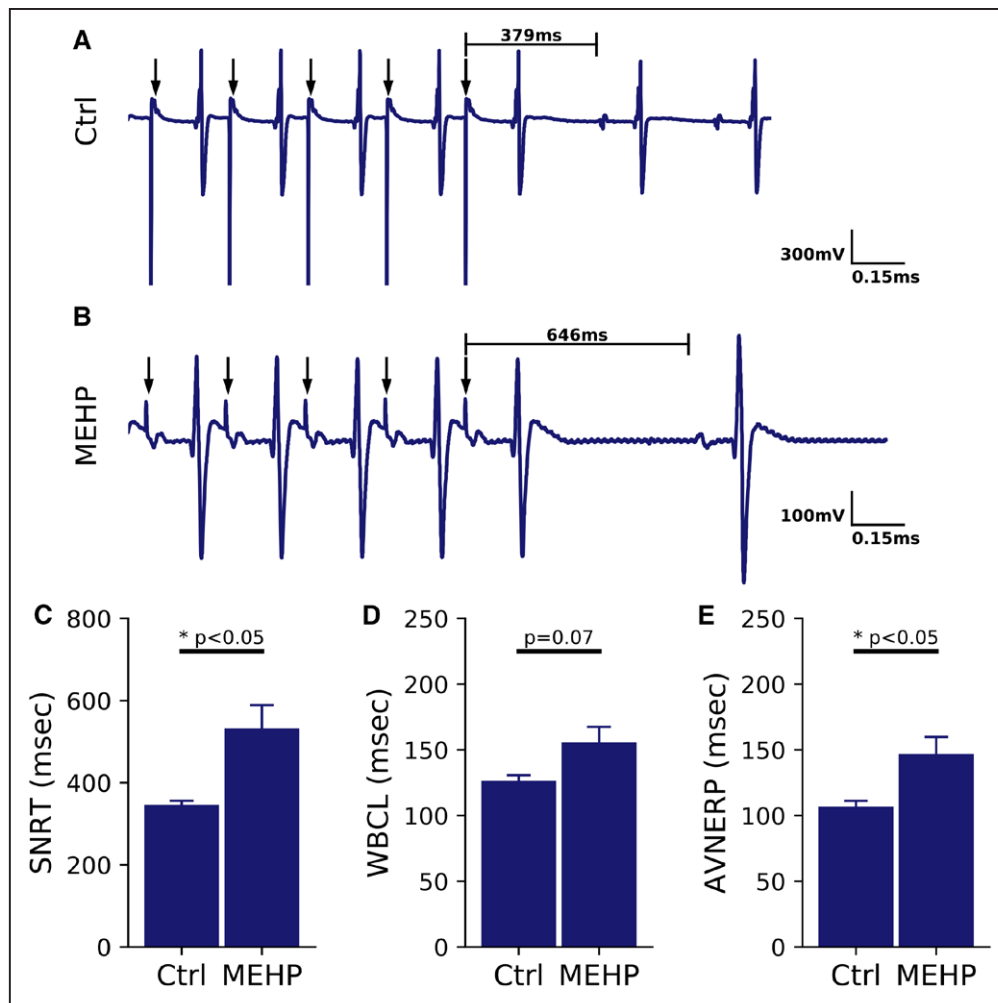


**Figure 2. Sinus node function and atrioventricular conduction altered after mono-2-ethylhexyl phthalate (MEHP) treatment.** **A**, ECG trace corresponding to a 200 ms pacing cycle length (PCL) train (indicated by arrows) on the right atrium in a control (Ctrl) heart. Sinus node recovery time (SNRT) is indicated as the delay between the cessation of pacing and the resumption of sinus node activity. **B**, SNRT measured in MEHP-treated heart shows marked prolongation compared with Ctrl. **C**, Aggregate SNRT analysis for MEHP-treated hearts and time-matched Ctrl ( $P<0.05$ ). **D**, Wenckebach cycle length (WBCL) measured as the earliest PCL in which Wenckebach phenomenon was visible ( $P=0.07$ ). **E**, Atrioventricular nodal refractory period (AVNERP) assessed by S1-S2 pacing on the right atrium was significantly lengthened in MEHP hearts compared with Ctrl ( $P<0.05$ ).  $n=5-8$  per group.

ure 1C and 1D). Beat rate variability was assessed as a cumulative index of automaticity and sinus node discharge. Although both root means successive square difference and SD of the normal RR intervals trended higher in MEHP-treated hearts ( $9.4\pm 2.4$  and  $17.3\pm 4.2$  ms, respectively) compared with controls ( $5.4\pm 1.7$  and  $11.9\pm 2.5$  ms, respectively), neither parameter was significant (root means successive square difference,  $P=0.19$ ; SD of the normal RR intervals,  $P=0.28$ ) Figures 1E and 1F. MEHP treatment increased  $RJ_{point}$  and RT intervals by 55% and 30%, respectively (Figure 2), both readily identifiable indicators of depolarization and repolarization in the excised rodent heart<sup>44</sup> (Figures 1G and 1H). Atrioventricular conduction delay was also measured during sinus rhythm. Atrioventricular conduction remained relatively stable in control hearts, as indicated by a PR interval time of  $43\pm 2$  ms at baseline and  $47\pm 2$  ms after 30-minute perfusion. In comparison, the PR interval time increased by 44%

in MEHP-treated hearts ( $41\pm 1$  ms baseline,  $59\pm 3$  ms,  $P<0.05$ ; Figure 1I).

### Electrophysiological Study

Sinus node function was further investigated by measuring sinus node recovery time, which was delayed by 54% in MEHP-treated hearts ( $532\pm 57$  ms) compared with control hearts ( $345\pm 10$  ms,  $P=0.01$ , Figure 2A through 2C). WBCL trended longer in MEHP-treated hearts compared with controls,  $155.8\pm 12.4$  to  $126.6\pm 4.5$  ( $P=0.07$ , Figure 2D). Atrioventricular node conduction refractoriness was interrogated by implementing an atrial pacing protocol to measure AVNERP, which was significantly longer in MEHP-treated hearts compared with controls,  $147\pm 13$  ms to  $107\pm 4.4$  ms ( $P<0.05$ , Figure 2E). These results suggest that MEHP may directly increase atrioventricular nodal refractoriness.



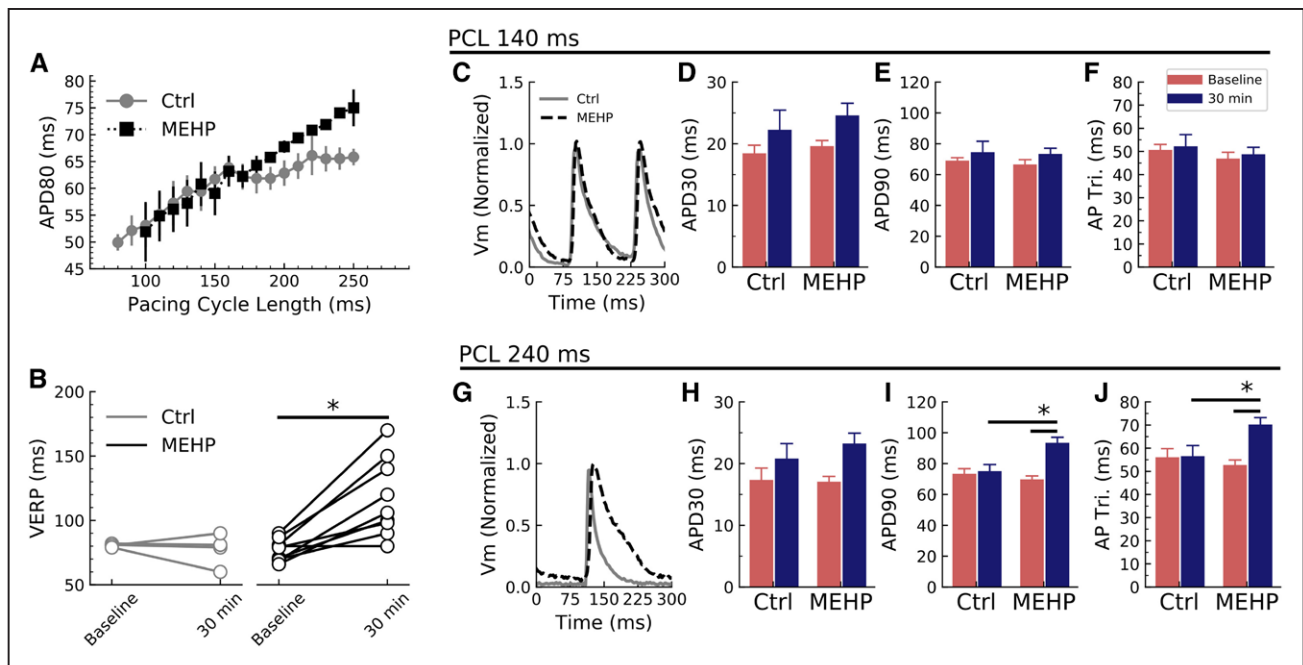


**Figure 3. Mono-2-ethylhexyl phthalate (MEHP) causes action potential morphology changes with corresponding modification of the electrical restitution curve.**

**A**, MEHP exposure caused the restitution curve to change from a biphasic form to a monophasic form with no plateau phase. The slope of the plateau on the control (Ctrl) heart was 0.06 compared with 0.18 in the MEHP hearts. **B**, Despite the similarities in the action potential duration at faster cycle lengths, the ventricular effective refractory period (VERP) was markedly prolonged in the MEHP-treated group ( $P < 0.05$ ). **C**, With rapid pacing (pacing cycle length [PCL]=140 ms), the action potential duration (APD) appeared similar between the Ctrl and MEHP-treated groups: there were no difference between **(D)** APD30, **(E)** APD90, or **(F)** AP triangulation. **G**, At slower cycle lengths (PCL=240 ms), the action potential morphology was quite different: while **(H)** APD30 was similar, **(I)** lengthening was apparent in the late phase as shown by APD90 ( $P < 0.05$ ). **J**, The effect on APD90 with no change on APD30 caused an increase in the triangulation shape of the AP after MEHP treatment ( $P < 0.05$ ).  $N=7$  for each group. AP Tri indicates action potential triangulation; and Vm, transmembrane voltage.

### Effects of MEHP Exposure on Ventricular Conduction and Refractoriness During Sinus Rhythm

ECG frequency content was also analyzed during sinus rhythm, as high frequencies during depolarization are associated with abnormal or slowed conduction.<sup>47,62</sup> In MEHP-treated hearts, contribution of high frequencies (400–500 Hz) was increased by 0.032% (interquartile range, -0.008% to 0.20%), whereas in control group, contribution of the same frequency band (400–500 Hz) decreased by 0.06% (interquartile range, 0.04%–1.19%),  $P=0.076$ . ECG lead placement among isolated hearts proved difficult due to the lack of anatomic markers and consistency in positioning of the heart relative to ECG leads, making experimental variability between individual hearts high for PSD measurements. Follow-up studies were performed using optical mapping, because APD and VERP measurements may more accurately predict alterations in ventricular repolarization in the rodent heart.<sup>63</sup>

### Effects of MEHP Exposure on Epicardial Conduction and Refractoriness During Epicardial Pacing

Optical mapping of transmembrane voltage signals was performed to evaluate action potential shape and dura-

tion, using an epicardial pacing protocol. APD at 80% repolarization (APD80) was assessed until VERP was reached, and APD80 values were compared between the timed control and MEHP-treatment group giving rise to the electrical restitution curves (Figure 3A). Ventricular refractoriness was determined during our optical mapping protocol which involves ventricular pacing at both baseline and 30-minute conditions. VERP was 51% longer in MEHP-treated hearts ( $117 \pm 9.5$  ms) compared with time-matched controls ( $77.5 \pm 5.5$  ms,  $P < 0.05$ ; Figure 3B). A longer refractory period suggests that MEHP exposure slows repolarization. MEHP-treated hearts displayed a monophasic restitution curve with a slope of 0.18 throughout (steep portion only, no plateau), as compared to controls which displayed a biphasic shape (steep and plateau phases). The steep slope of the controls was like that of the MEHP group at 0.17, and the slope of the plateau phase was 0.06. Importantly, monophasic restitution curves are associated with an increased risk of electrical alternans.<sup>54,64</sup> With a lengthened VERP in MEHP-treated hearts, loss of capture at PCLs <100 ms limited APD measurements in the MEHP group.

APD30 and APD90 were measured to compute the triangulation of the action potential. At a selected fast PCL (140 ms), there were no significant differences between control and MEHP (Figure 3C). APD30

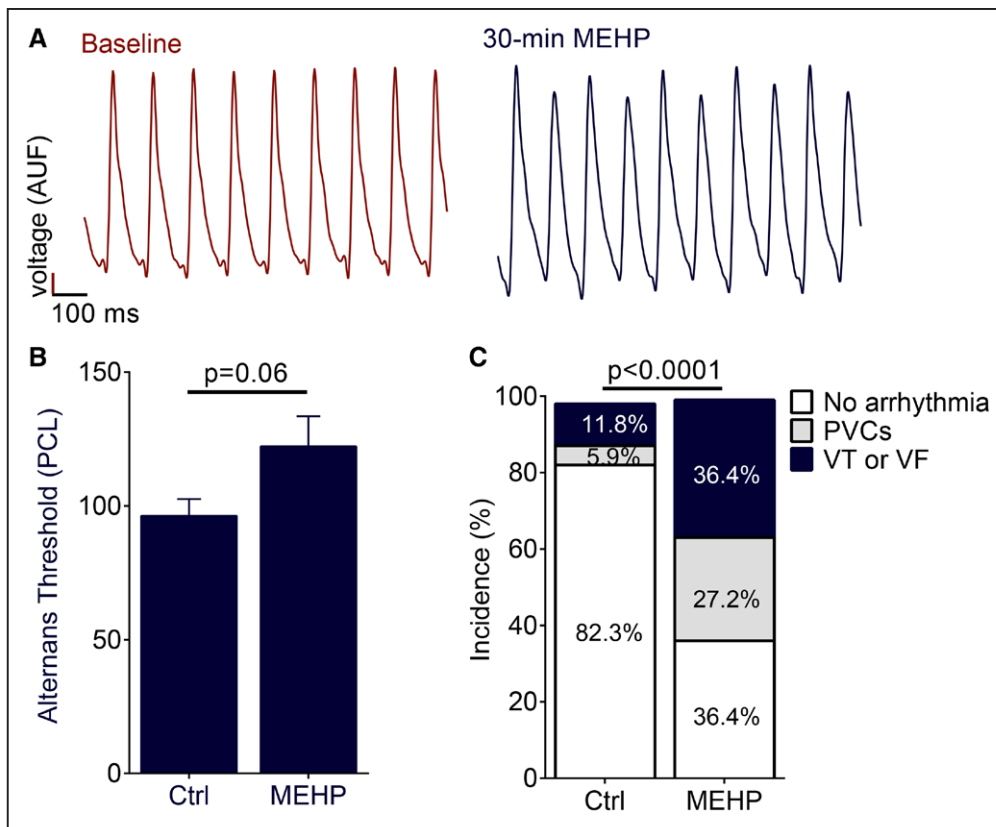


**Figure 4. Action potential alternans and arrhythmia susceptibility from mono-2-ethylhexyl phthalate (MEHP) exposure.**

**A**, MEHP-treated hearts displayed increased susceptibility to alternating action potential morphology at the same pacing cycle length (PCL) compared with baseline as predicted by the change in electrical restitution (See Figure 3A), PCL=110 ms this example. **B**, The longest PCL which resulted in alternating action potentials (alternans threshold) was longer in the MEHP-treated hearts ( $P=0.06$ ). **C**, Hearts after MEHP exposure became more susceptible to spontaneous arrhythmia as shown by a higher incidence of both premature ventricular contractions (PVC) and ventricular tachycardia or ventricular fibrillation (VT/VF) following electrophysiological study ( $P<0.0001$ ,  $\chi^2$  test).  $N=8$  for each group. AUF indicates arbitrary units of fluorescence; and Ctrl, control.

prolonged with time in both groups (Figure 3D), with no difference between APD90 and AP triangulation (Figures 3E and 3F, respectively). At a slower PCL (240 ms), APD90 was significantly prolonged in MEHP-treated hearts ( $93.5\pm 3.5$  ms) compared with controls ( $75.2\pm 4.2$  ms,  $P=0.02$ ) (Figure 3G). The lengthening of APD90 (Figure 3I) without a significant change in APD30 (Figure 3H) led to an increase in the AP triangulation ( $APD90-APD30$ )<sup>53</sup>; AP triangulation was  $56.6\pm 4.5$  ms in the controls and increased to  $70.3\pm 2.9$  ms in the MEHP group (Figure 3J). These results suggest that MEHP exposure exerts a reverse use-dependence effect, wherein myocyte refractoriness and action potential prolongation is increased at slower heart rates.<sup>65</sup>

### Electrical Alternans and Arrhythmia Susceptibility

AP triangulation, reverse use dependence, and a monophasic electrical restitution curve with no plateau phase have been associated with an increased propensity for electrical alternans and arrhythmias.<sup>53,54,66</sup> APD instability was assessed by quantifying the incidence of electrical

alternans or sequential beat-to-beat variations in APD, such as displayed in Figure 4A. The threshold of electrical alternans was observed in MEHP-treated hearts at a cycle length of  $122\pm 11$  ms compared with  $96\pm 6$  ms PCL ( $P=0.06$ , Figure 4B). Rodent hearts are resistant to fibrillation, due in part to the small tissue mass.<sup>44</sup> Therefore, to assess arrhythmia susceptibility, each individual heart was scored by the most severe electrical disturbance encountered during the electrophysiology study at the end of the experiment. Arrhythmia incidence was significantly increased in MEHP-treated hearts, compared with controls ( $P<0.05$ , Figure 4C).

### MEHP Exposure Slows Conduction Velocity

Our previous in vitro studies suggest that phthalate esters uncouple neighboring cardiomyocytes, resulting in slowed conduction and an arrhythmogenic phenotype.<sup>40</sup> To test whether this effect was observed in an intact heart, CV across the epicardial surface was measured using optical mapping and a unipolar, cathodal pacing electrode. The electrode was centered in the field of view, and  $10^\circ$  increments were used to measure

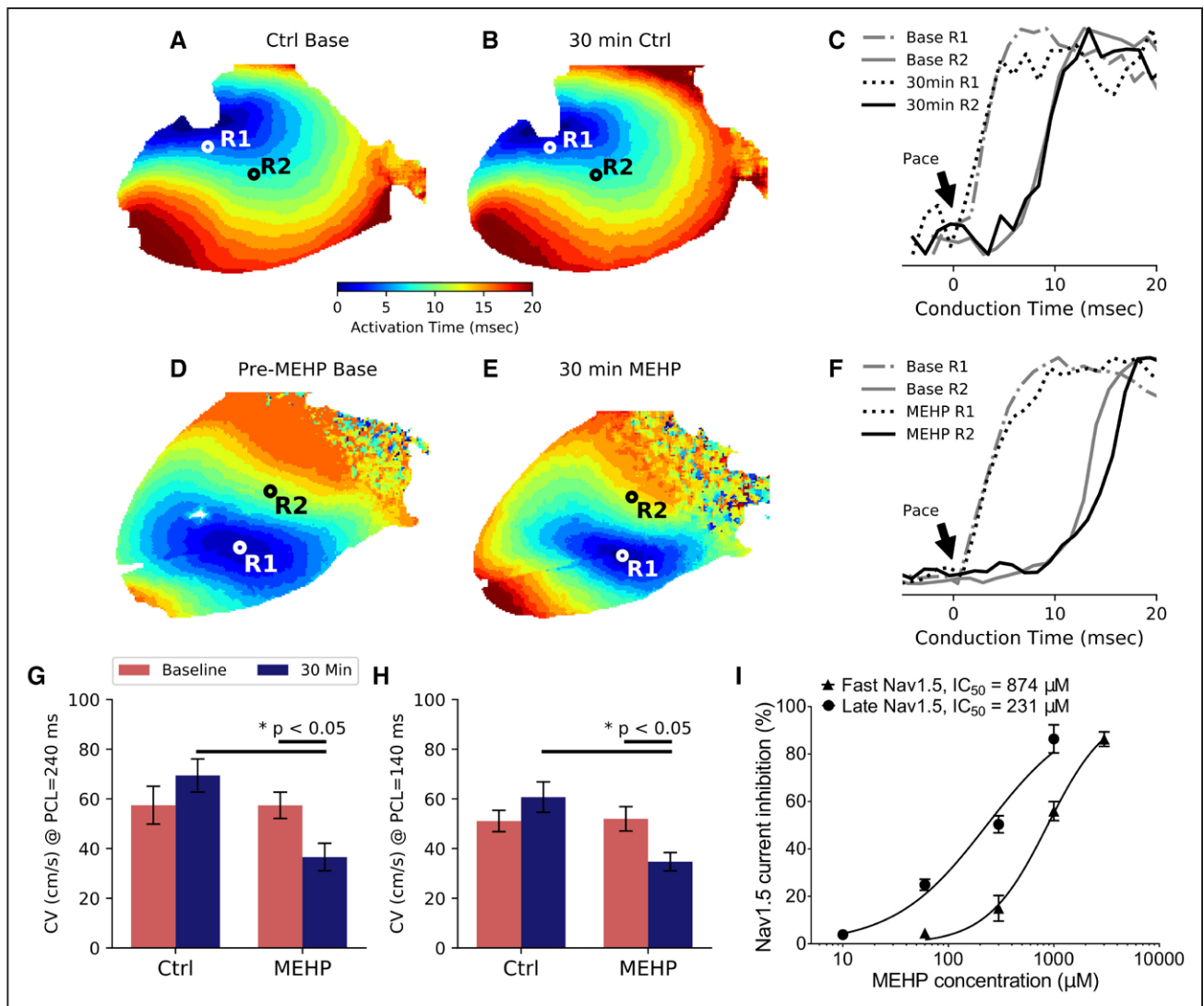


**Figure 5. Activation maps and measured conduction velocity (CV) after mono-2-ethylhexyl phthalate (MEHP) exposure.**

**A**, Each pixel on the heart was assigned an activation time based on the maximum upstroke velocity in the fluorescent signal to create an isochrone map. Wavefronts are visible emanating from the center of the left ventricular epicardium where the cathodal pacing electrode was placed. **B**, After 30-min control (Ctrl)-media perfusion, the activation maps did not show significant differences. **C**, In Ctrl hearts, analysis of the pacing site (R1) and a distal site (R2) did not show significant differences in conduction time when compared between baseline and 30-min perfusion. **D**, Pre-MEHP baseline showed similar CV as the Ctrl baseline. **E**, After 30-min of MEHP exposure, the activation maps changed in morphology. **F**, Analysis of the pacing site (R1) and distal site (R2) indicated a decreased upstroke velocity after 30-min of MEHP exposure. **G**, CV was significantly slower in MEHP-treated hearts compared with Ctrl hearts after 30 min at both pacing cycle length (PCL)=240 ms ( $P<0.05$ ) and **(H)** PCL=140 ms ( $P<0.05$ ), with N=5 per group. **I**, Sodium current ( $I_{Na}$ ) was measured with HEK293 (human embryonic kidney 293) cells which stably express  $Na_v1.5$ . Fast sodium current ( $I_{NaF}$ ) was measured in the absence of anemone toxin, and half-maximal inhibition concentration ( $IC_{50}$ ) was determined at 874  $\mu\text{mol/L}$ . Late sodium current ( $I_{NaL}$ ) was activated with anemone toxin, and corresponding  $IC_{50}$  was determined at 231  $\mu\text{mol/L}$  (N=5 for each group).

$\geq 180^\circ$  of coverage for longitudinal and transverse CV measurements. Optical mapping confirmed that paced beats propagated as elliptical wavefronts that emanated from the pacing electrode (Figures 5A through 5D). For depiction, we show 2 selected regions for each heart across the epicardial surface and the conduction time from pacing initiation to the distal site under control (Figure 5E) and MEHP (Figure 5F) conditions. To investigate CV restitution, both a slow (240 ms) and fast (140 ms) PCL were selected for CV measurements. Incidentally, CV increased slightly between baseline and 30-minute timed recordings in control hearts at both pacing rates (Figures 5G and 5H). However, MEHP-

treated hearts displayed 47% slower CV at 240 ms PCL (Figure 5G) and 42% slower CV at 140 ms PCL (Figure 5H) compared with time-matched controls.

### MEHP Inhibits Sodium Channel Current

Slowed myocardial CV can be attributed to a reduction in sodium channel current, anatomic obstacles, or diminished cellular coupling (eg, gap junctions). Because the latter 2 mechanisms may take additional time (exceeding 30-minute chemical exposure), we focused our attention on the direct effects of MEHP on sodium current. The onset of current suppression

was concentration-dependent (Figure 5I). MEHP suppressed fast and late sodium current ( $I_{Na}$ ) with an IC<sub>50</sub> of 874  $\mu\text{mol/L}$  and 231  $\mu\text{mol/L}$ , respectively. Tetrodotoxin (30  $\mu\text{mol/L}$ ), a potent neurotoxin that blocks Nav1.5, served as a positive control resulting in >96% inhibition for all experiments (data not shown). Using in silico modeling combined with IC<sub>50</sub> values, 60  $\mu\text{M}$  MEHP is expected to decrease  $dV/dt$  by 4.6% (215 to 205 mV/ms), based on a human epicardial action potential at basic cycle length of 250 ms.

## DISCUSSION

This study is the first to examine the impact of MEHP on the electrophysiology of the intact heart, using a clinically relevant concentration that was comparable to patient exposure after an exchange transfusion procedure<sup>13</sup> or measured levels in stored blood products.<sup>4,42</sup> Importantly, we show that acute MEHP exposure results in slowed atrioventricular conduction, slowed epicardial CV, and increased atrioventricular and ventricular refractory periods. Optical mapping studies revealed a prolonged APD at slower PCLs, akin to reverse use dependence. MEHP-treated hearts also displayed a triangulated action potential and a steeper electrical restitution curve—both of which have been associated with an increased propensity for electrical alternans and arrhythmias.

### Automaticity and Sinus Node Function

Automaticity in the isolated heart is determined by a balance between inward and outward currents (voltage clock)<sup>67–69</sup> and calcium oscillations (calcium clock),<sup>70</sup> and as such, alterations in the spontaneous beating rate can serve as a cumulative index of cardiac excitability. Previous studies have reported bradycardia after phthalate exposure in vivo<sup>39</sup> (>20 mg/kg MEHP), in vitro<sup>71</sup> (10  $\mu\text{M}$  DEHP), and using an isolated heart model<sup>72</sup> (250  $\mu\text{M}$  DEHP). In the current study, we observed comparable heart rates between treatment groups (control, MEHP) at the dose and duration chosen for the study (60  $\mu\text{M}$  MEHP, 30 minutes). Alterations in automaticity may become more pronounced after longer treatment times, with higher concentrations, or exposure to the parent compound versus metabolite (DEHP versus MEHP). We also examined beat rate variability as a cumulative index of automaticity and sinus node discharge. Both root means successive square difference and SD of the normal RR intervals trended higher in MEHP-treated hearts, but neither parameter was statistically significant. Sinus node function was directly measured using a pacing protocol to quantify sinus node recovery time, which was significantly delayed by 54% in MEHP-treated hearts. These results suggest an underlying effect of phthalate esters on potassium

channel current or calcium handling in the sinoatrial node<sup>74</sup>; indeed, alterations in calcium cycling and contractility have been reported in cardiac preparations treated with phthalate esters.<sup>36,41</sup>

### Atrioventricular Conduction

We assessed the direct effect of MEHP exposure on intrinsic atrioventricular electrical conduction, by quantifying PR interval, AVNERP, and WBCL. Similar to a previous report by Aronson et al,<sup>72</sup> we observed a 44% prolongation of PR interval time in MEHP-treated hearts compared with controls—concomitant with a 37% increase in AVNERP and 23% increase in WBCL. Negative dromotropy through the atrioventricular node is commonly observed with cholinergics, and at least 1 study has shown that the effects of phthalate esters on human atrial trabeculae are partially inhibited by atropine, suggesting an interaction with cholinergic receptors.<sup>36</sup> Alternatively, an interaction between phthalate esters and potassium or calcium channels could also alter nodal conduction. Indeed, a recent whole-cell patch clamp study demonstrated that phthalate exposure (10–100  $\mu\text{M}$  DEHP, parent compound of MEHP) blocks L-type calcium channels in vascular smooth muscle cells.<sup>74</sup>

### Ventricular Conduction and Electrical Instability

Using an isolated intact heart preparation, we observed significant effects on ventricular conduction and repolarization. During sinus rhythm, MEHP-treatment prolonged  $RJ_{\text{point}}$  and RT intervals, indicating a slowing of the internal conduction system. Notably, recent studies have highlighted the utility of APD and VERP measurements as precise indicators of ventricular repolarization.<sup>63</sup> Using an epicardial pacing protocol, we observed a 51% increase in VERP and 24% increase in APD<sub>90</sub> time at slower PCL. On the surface, this result might suggest a beneficial, antiarrhythmic effect of acute MEHP exposure. Though importantly, APD prolongation is a key contributor to electrical instability when the AP is triangulated<sup>53,66</sup>—as is the case with pharmaceuticals that exert off-target effects on potassium channels encoded by *hERG*, which can set the stage for early afterdepolarizations and Torsades.<sup>75</sup> Moreover, reverse-use dependence can also be proarrhythmic as the APD restitution slope changes shape and becomes steeper. Similar to the effects of sotalol on electrical restitution,<sup>76</sup> we observed significant APD<sub>90</sub> prolongation at slower PCL (>190 ms) and a steep, monophasic APD restitution curve in MEHP-treated hearts. A steeper APD restitution slope with lack of plateau phase at longer basic cycle lengths can lead to an increased spatial dispersion of restitution properties, therefore, creating a proarrhythmic milieu



and electrical alternans.<sup>64</sup> Due to a significant difference in VERP, we were unable to reach faster pacing rates in MEHP-treated hearts, but electrical alternans were observed at longer PCL in MEHP hearts (122 ms) compared with controls (96 ms). We also observed a 42% to 47% decrease in epicardial CV, which can be partly attributed to an immediate inhibitory effect of MEHP on sodium channels. Indeed, fast and late sodium channel current was inhibited by MEHP (IC<sub>50</sub> 874 μmol/L and 231 μmol/L MEHP, respectively) using a HEK293 cell line stably expressing Na<sub>v</sub>1.5. IC<sub>50</sub> values were subsequently used for human in silico modeling, predicting a modest slowing of dV/dt. Though the latter was more modest than anticipated, additional voltage-clamp studies using a cardiomyocyte model may aid in the interpretation of these results.

Due to the acute nature of the observed effects of MEHP exposure, our study suggests that phthalate esters interfere with ionic currents in the myocardium—and these effects may be multifactorial. Unfortunately, the rodent myocardium is not ideal for assessing arrhythmia incidence because of its small size and robustness to fibrillation.<sup>44</sup> Future electrophysiological studies are needed, in a larger animal model, to definitively draw a conclusion on the arrhythmogenic potential of MEHP and other phthalate esters. Clinical studies showed that abnormal slow conduction in patients with ventricular arrhythmias can manifest by increased power of high frequencies within the ECG signal.<sup>62,77</sup> In this study, we observed a trend towards higher contribution of high frequencies within QRS, but PSD measurements proved difficult due to variability in excised heart positioning relative to ECG lead placement.

## Study Limitations

The scope of the study was limited to the effect of acute (30 minutes) MEHP exposure on cardiac electrophysiology, using an isolated heart model. Such a model prevents the investigation of longer exposure time, and ex vivo results may differ from in vivo studies with an intact vascular and autonomic nervous system. The reported results are also limited to the effect of MEHP, and therefore, do not account for additional effects that may be caused by DEHP (the parent compound) or other secondary metabolites. The presented study was also limited to a single dose of MEHP, which was chosen based on the reported blood concentration after an exchange transfusion procedure.

## Conclusions

This study reports the electrophysiological effects of MEHP on intact, isolated rodent hearts. The increase in action potential triangulation and altered APD restitution curve are both indicators of increased arrhythmic risk.

## ARTICLE INFORMATION

Received February 12, 2019; accepted April 22, 2019.

### Correspondence

Nikki Gillum Posnack, PhD, Sheikh Zayed Institute, 6th floor, M7708, 111 Michigan Ave, NW, Washington DC 20010. Email nposnack@childrensnational.org

### Affiliations

Sheikh Zayed Institute for Pediatric Surgical Innovation (R.J., D. McCullough, L.S., D. McInerney, J.H., N.G.P.) and Children's National Heart Institute (R.J., B.S., L.S., N.G.P.), Children's National Health System, Washington DC. Departments of Pediatrics and Pharmacology and Physiology, School of Medicine and Health Sciences: George Washington University, Washington DC (N.G.P.). CiPA Lab, LLC, Rockville, MD (J.S.). Ci2B-Universitat Politècnica de València, Spain (B.T., F.J.S.R.). Knight Cardiovascular Institute, Oregon Health and Science University, Portland (E.A.P.-A., L.G.T.).

### Acknowledgments

We gratefully acknowledge Manelle Ramadan, BS, Morgan Burke, BS, and Ashish Doshi, MD, PhD for technical assistance.

### Sources of Funding

This work was supported by the National Institutes of Health (R00ES023477 and R01HL139472 to Dr Posnack), Children's Research Institute and Children's National Heart Institute. We thank the generosity of the NVIDIA corporation for the graphics processing unit to perform image processing. This work was partially supported by the Dirección General de Política Científica de la Generalitat Valenciana (PROMETEU2016/088) to J.S. and B.T.

### Disclosures

None.

## REFERENCES

- Braun JM, Sathyanarayana S, Hauser R. Phthalate exposure and children's health. *Curr Opin Pediatr*. 2013;25:247–254. doi: 10.1097/MOP.0b013e32835e1eb6
- Luban N, Rais-Bahrami K, Short B. I want to say one word to you—just one word—“plastics”. *Transfusion*. 2006;46:503–506. doi: 10.1111/j.1537-2995.2006.00766.x
- van der Meer PF, Reesink HW, Panzer S, Wong J, Ismay S, Keller A, Pink J, Buchta C, Compennolle V, Wendel S, Biagini S, Scuracchio P, Thibault L, Germain M, Georgsen J, Bégué S, Dernis D, Raspollini E, Villa S, Rebullia P, Takashi M, de Korte D, Lozano M, Cid J, Gulliksson H, Cardigan R, Tooke C, Fung MK, Luban NL, Vassallo R, Benjamin R. Should DEHP be eliminated in blood bags? *Vox Sang*. 2014;106:176–195. doi: 10.1111/vox.12099
- FDA. Safety Assessment of Di(2-ethylhexyl)phthalate (DEHP) Released from PVC Medical Devices [Internet]. [https://noharm-uscanada.org/sites/default/files/documents-files/116/Safety\\_Assessment\\_of\\_DEHP.pdf](https://noharm-uscanada.org/sites/default/files/documents-files/116/Safety_Assessment_of_DEHP.pdf).
- Loff S, Kabs F, Witt K, Sartoris J, Mandl B, Niessen KH, Waag KL. Polyvinylchloride infusion lines expose infants to large amounts of toxic plasticizers. *J Pediatr Surg*. 2000;35:1775–1781. doi: 10.1053/jpsu.2000.19249
- Rais-Bahrami K, Nunez S, Revenis ME, Luban LC, Short BL. Adolescents exposed to DEHP in plastic tubing as neonates: research briefs. *Pediatr Nurs*. 2004;30:406–433.
- Mallow EB, Fox MA. Phthalates and critically ill neonates: device-related exposures and non-endocrine toxic risks. *J Perinatol*. 2014;34:892–897. doi: 10.1038/jp.2014.157
- Sjöberg P, Bondesson U, Sedin G, Gustafsson J. Dispositions of di- and mono-(2-ethylhexyl) phthalate in newborn infants subjected to exchange transfusions. *Eur J Clin Invest*. 1985;15:430–436.
- Barry YA, Labow RS, Keon WJ, Tocchi M, Rock G. Perioperative exposure to plasticizers in patients undergoing cardiopulmonary bypass. *J Thorac Cardiovasc Surg*. 1989;97:900–905.
- Peck CC, Odom DG, Friedman HI, Albro PW, Hass JR, Brady JT, Jess DA. Di-2-ethylhexyl phthalate (DEHP) and mono-2-ethylhexyl phthalate (MEHP) accumulation in whole blood and red cell concentrates. *Transfusion*. 1979;19:137–146.

11. Pollack GM, Buchanan JF, Slaughter RL, Kohli RK, Shen DD. Circulating concentrations of di(2-ethylhexyl) phthalate and its de-esterified phthalic acid products following plasticizer exposure in patients receiving hemodialysis. *Toxicol Appl Pharmacol.* 1985;79:257–267.
12. Faouzi MA, Dine T, Gressier B, Kambia K, Luyckx M, Pagniez D, Brunet C, Cazin M, Belabed A, Cazin JC. Exposure of hemodialysis patients to di-2-ethylhexyl phthalate. *Int J Pharm.* 1999;180:113–121.
13. Sjöberg PO, Bondesson UG, Sedin EG, Gustafsson JP. Exposure of newborn infants to plasticizers. Plasma levels of di-(2-ethylhexyl) phthalate and mono-(2-ethylhexyl) phthalate during exchange transfusion. *Transfusion.* 1985;25:424–428.
14. Shneider B, Schena J, Truog R, Jacobson M, Keyv S. Exposure to di(2-ethylhexyl)phthalate in infants receiving extracorporeal membrane oxygenation. *N Engl J Med.* 1989;320:1563. doi: 10.1056/NEJM198906083202323
15. Karle VA, Short BL, Martin GR, Bulas DI, Getson PR, Luban NL, O'Brien AM, Rubin RJ. Extracorporeal membrane oxygenation exposes infants to the plasticizer, di(2-ethylhexyl)phthalate. *Crit Care Med.* 1997;25:696–703.
16. Plonait SL, Nau H, Maier RF, Wittfoht W, Obladen M. Exposure of newborn infants to di-(2-ethylhexyl)-phthalate and 2-ethylhexanoic acid following exchange transfusion with polyvinylchloride catheters. *Transfusion.* 1993;33:598–605.
17. Gaynor JW, Ittenbach RF, Calafat AM, Burnham NB, Bradman A, Bellinger DC, Henretig FM, Wehrung EE, Ward JL, Russell WW, Spray TL. Perioperative exposure to suspect neurotoxicants from medical devices in newborns with congenital heart defects. *Ann Thorac Surg.* 2019;107:567–572. doi: 10.1016/j.athoracsur.2018.06.035
18. Calafat AM, Needham LL, Silva MJ, Lambert G. Exposure to di-(2-ethylhexyl) phthalate among premature neonates in a neonatal intensive care unit. *Pediatrics.* 2004;113:e429–e434.
19. Demirel A, Çoban A, Yıldırım Ş, Doğan C, Sancı R, İnce Z. Hidden toxicity in neonatal intensive care units: phthalate exposure in very low birth weight infants. *J Clin Res Pediatr Endocrinol.* 2016;8:298–304. doi: 10.4274/jcrpe.3027
20. Su PH, Chang YZ, Chang HP, Wang SL, Haung HI, Huang PC, Chen JY. Exposure to di(2-ethylhexyl) phthalate in premature neonates in a neonatal intensive care unit in Taiwan. *Pediatr Crit Care Med.* 2012;13:671–677. doi: 10.1097/PCC.0b013e3182455558
21. Huygh J, Clotman K, Malarvannan G, Covaci A, Schepens T, Verbrugghe W, Dirinck E, Van Gaal L, Jorens PG. Considerable exposure to the endocrine disrupting chemicals phthalates and bisphenol-A in intensive care unit (ICU) patients. *Environ Int.* 2015;81:64–72. doi: 10.1016/j.envint.2015.04.008
22. Koch HM, Preuss R, Angerer J. Di(2-ethylhexyl)phthalate (DEHP): human metabolism and internal exposure— an update and latest results. *Int J Androl.* 2006;29:155–165; discussion 181. doi: 10.1111/j.1365-2605.2005.00607.x
23. Kessler W, Numtip W, Völkel W, Seckin E, Csanády GA, Pütz C, Klein D, Fromme H, Filser JG. Kinetics of di(2-ethylhexyl) phthalate (DEHP) and mono(2-ethylhexyl) phthalate in blood and of DEHP metabolites in urine of male volunteers after single ingestion of ring-deuterated DEHP. *Toxicol Appl Pharmacol.* 2012;264:284–291. doi: 10.1016/j.taap.2012.08.009
24. Casals-Casas C, Desvergne B. Endocrine disruptors: from endocrine to metabolic disruption. *Annu Rev Physiol.* 2011;73:135–162. doi: 10.1146/annurev-physiol-012110-142200
25. Diamanti-Kandarakis E, Bourguignon JP, Giudice LC, Hauser R, Prins GS, Soto AM, Zoeller RT, Gore AC. Endocrine-disrupting chemicals: an Endocrine Society scientific statement. *Endocr Rev.* 2009;30:293–342. doi: 10.1210/er.2009-0002
26. Halden RU. Plastics and health risks. *Annu Rev Public Health.* 2010;31:179–194. doi: 10.1146/annurev.publhealth.012809.103714
27. Swan SH. Prenatal phthalate exposure and anogenital distance in male infants. *Environ Health Perspect.* 2006;114:A88–A89. doi: 10.1289/ehp.114-a88b
28. Tickner JA, Schettler T, Guidotti T, McCally M, Rossi M. Health risks posed by use of Di-2-ethylhexyl phthalate (DEHP) in PVC medical devices: a critical review. *Am J Ind Med.* 2001;39:100–111.
29. Trasande L, Sathyanarayanan S, Spanier AJ, Trachtman H, Attina TM, Urbina EM. Urinary phthalates are associated with higher blood pressure in childhood. *J Pediatr.* 2013;163:747–53.e1. doi: 10.1016/j.jpeds.2013.03.072
30. von Rettberg H, Hannman T, Subotic U, Brade J, Schaible T, Waag KL, Loff S. Use of di(2-ethylhexyl)phthalate-containing infusion systems increases the risk for cholestasis. *Pediatrics.* 2009;124:710–716. doi: 10.1542/peds.2008-1765
31. Kardas F, Bayram AK, Demirci E, Akin L, Ozmen S, Kendirci M, Canpolat M, Oztot DB, Narin F, Gumus H, Kumandas S, Per H. Increased serum phthalates (MEHP, DEHP) and bisphenol A concentrations in children with autism spectrum disorder: the role of endocrine disruptors in autism etiopathogenesis. *J Child Neurol.* 2016;31:629–635. doi: 10.1177/0883073815609150
32. Green R, Hauser R, Calafat AM, Weuve J, Schettler T, Ringer S, Huttner K, Hu H. Use of di(2-ethylhexyl) phthalate-containing medical products and urinary levels of mono(2-ethylhexyl) phthalate in neonatal intensive care unit infants. *Environ Health Perspect.* 2005;113:1222–1225. doi: 10.1289/ehp.7932
33. Calafat AM, Weuve J, Ye X, Jia LT, Hu H, Ringer S, Huttner K, Hauser R. Exposure to bisphenol A and other phenols in neonatal intensive care unit premature infants. *Environ Health Perspect.* 2009;117:639–644. doi: 10.1289/ehp.0800265
34. Sampson J, de Korte D. DEHP-plasticized PVC: relevance to blood services. *Transfus Med.* 2011;21:73–83. doi: 10.1111/j.1365-3148.2010.01056.x
35. Barry YA, Labow RS, Rock G, Keon WJ. Cardiotoxic effects of the plasticizer metabolite, mono (2-ethylhexyl)phthalate (MEHP), on human myocardium. *Blood.* 1988;72:1438–1439.
36. Barry YA, Labow RS, Keon WJ, Tocchi M. Atropine inhibition of the cardiodepressive effect of mono(2-ethylhexyl)phthalate on human myocardium. *Toxicol Appl Pharmacol.* 1990;106:48–52.
37. Jaimes R III, Swiercz A, Sherman M, Muselimyan N, Marvar PJ, Posnack NG. Plastics and cardiovascular health: phthalates may disrupt heart rate variability and cardiovascular reactivity. *Am J Physiol Heart Circ Physiol.* 2017;313:H1044–H1053. doi: 10.1152/ajpheart.00364.2017
38. Labow RS, Barry YA, Tocchi M, Keon WJ. The effect of mono(2-ethylhexyl) phthalate on an isolated perfused rat heart-lung preparation. *Environ Health Perspect.* 1990;89:189–193. doi: 10.1289/ehp.9089189
39. Rock G, Labow RS, Franklin C, Burnett R, Tocchi M. Hypotension and cardiac arrest in rats after infusion of mono(2-ethylhexyl)phthalate (MEHP), a contaminant of stored blood. *N Engl J Med.* 1987;316:1218–1219. doi: 10.1056/NEJM198705073161915
40. Gillum N, Karabekian Z, Swift LM, Brown RP, Kay MW, Sarvazyan N. Clinically relevant concentrations of di (2-ethylhexyl) phthalate (DEHP) uncouple cardiac syncytium. *Toxicol Appl Pharmacol.* 2009;236:25–38. doi: 10.1016/j.taap.2008.12.027
41. Posnack NG, Idrees R, Ding H, Jaimes R III, Stybayeva G, Karabekian Z, Laflamme MA, Sarvazyan N. Exposure to phthalates affects calcium handling and intercellular connectivity of human stem cell-derived cardiomyocytes. *PLoS One.* 2015;10:e0121927. doi: 10.1371/journal.pone.0121927
42. Rael LT, Bar-Or R, Ambruso DR, Mains CW, Slone DS, Craun ML, Bar-Or D. Phthalate esters used as plasticizers in packed red blood cell storage bags may lead to progressive toxin exposure and the release of pro-inflammatory cytokines. *Oxid Med Cell Longev.* 2009;2:166–171.
43. Jaimes R III, Kuzmiak-Glancy S, Brooks DM, Swift LM, Posnack NG, Kay MW. Functional response of the isolated, perfused normoxic heart to pyruvate dehydrogenase activation by dichloroacetate and pyruvate. *Pflügers Arch - Eur J Physiol.* 2016;468:131–142. doi:10.1007/s00424-015-1717-1
44. Boukens BJ, Rivaud MR, Rentschler S, Coronel R. Misinterpretation of the mouse ECG: 'musing the waves of Mus musculus'. *J Physiol.* 2014;592:4613–4626. doi: 10.1113/jphysiol.2014.279380
45. Erickson JR, Pereira L, Wang L, Han G, Ferguson A, Dao K, Copeland RJ, Despa F, Hart GW, Ripplinger CM, Bers DM. Diabetic hyperglycaemia activates CaMKII and arrhythmias by O-linked glycosylation. *Nature.* 2013;502:372–376. doi: 10.1038/nature12537
46. Perez-Alday EA, Li-Pershing Y, Bender A, Hamilton C, Thomas JA, Johnson K, Lee TL, Gonzales R, Li A, Newton K, Tereshchenko LG. Importance of the heart vector origin point definition for an ECG analysis: the Atherosclerosis Risk in Communities (ARIC) study. *Comput Biol Med.* 2019;104:127–138. doi: 10.1016/j.combiomed.2018.11.013
47. Sedaghat G, Gardner RT, Kabir MM, Ghafoori E, Habecker BA, Tereshchenko LG. Correlation between the high-frequency content of the QRS on murine surface electrocardiogram and the sympathetic nerves density in left ventricle after myocardial infarction: experimental study. *J Electrocardiol.* 2017;50:323–331. doi: 10.1016/j.jelectrocard.2017.01.014
48. Rempelmann O, Ros HH. Coherent averaging technique: a tutorial review. Part 1: noise reduction and the equivalent filter. *J Biomed Eng.* 1986;8:24–29.
49. Welch P. The use of fast fourier transform for the estimation of power spectra: a method based on time averaging over short, modified periodograms. *IEEE Trans Audio Electroacoust.* 1967;15:70–73.
50. Swift LM, Asfour H, Posnack NG, Arutunyan A, Kay MW, Sarvazyan N. Properties of blebbistatin for cardiac optical mapping and other imaging applications. *Pflügers Arch.* 2012;464:503–512. doi: 10.1007/s00424-012-1147-2



51. Kay M, Swift L, Martell B, Arutunyan A, Sarvazyan N. Locations of ectopic beats coincide with spatial gradients of NADH in a regional model of low-flow reperfusion. *Am J Physiol Heart Circ Physiol*. 2008;294:H2400–H2405. doi: 10.1152/ajpheart.01158.2007
52. Posnack NG, Jaimes R III, Asfour H, Swift LM, Wengrowski AM, Sarvazyan N, Kay MW. Bisphenol A exposure and cardiac electrical conduction in excised rat hearts. *Environ Health Perspect*. 2014;122:384–390. doi: 10.1289/ehp.1206157
53. Hondeghem LM, Carlsson L, Duker G. Instability and triangulation of the action potential predict serious proarrhythmia, but action potential duration prolongation is antiarrhythmic. *Circulation*. 2001;103:2004–2013.
54. Franz MR. The electrical restitution curve revisited: steep or flat slope—which is better? *J Cardiovasc Electrophysiol*. 2003;14(10 suppl):S140–S147.
55. Laughner JJ, Ng FS, Sulkin MS, Arthur RM, Efimov IR. Processing and analysis of cardiac optical mapping data obtained with potentiometric dyes. *Am J Physiol Heart Circ Physiol*. 2012;303:H753–H765. doi: 10.1152/ajpheart.00404.2012
56. Doshi AN, Walton RD, Krul SP, de Groot JR, Bernus O, Efimov IR, Boukens BJ, Coronel R. Feasibility of a semi-automated method for cardiac conduction velocity analysis of high-resolution activation maps. *Comput Biol Med*. 2015;65:177–183. doi: 10.1016/j.combiomed.2015.05.008
57. Hunter JD. Matplotlib: a 2D graphics environment. *Comput Sci Eng*. 2007;9:90–95.
58. Mantegazza M, Franceschetti S, Avanzini G. Anemone toxin (ATX II)-induced increase in persistent sodium current: effects on the firing properties of rat neocortical pyramidal neurones. *J Physiol*. 1998;507(pt 1):105–116.
59. O'Hara T, Virág L, Varró A, Rudy Y. Simulation of the undiseased human cardiac ventricular action potential: model formulation and experimental validation. *PLoS Comput Biol*. 2011;7:e1002061. doi: 10.1371/journal.pcbi.1002061
60. Grandi E, Sobie EA, Clancy CE, Li Z, Colatsky T, Dutta S, Chang KC, Beattie KA, Sheng J, Tran PN, Wu WW, Wu M, Strauss DG. Optimization of an in silico cardiac cell model for proarrhythmia risk assessment. *Front Physiol*. 2017;8:616.
61. Romero L, Cano J, Gomis-Tena J, Trenor B, Sanz F, Pastor M, Saiz J. In silico QT and APD prolongation assay for early screening of drug-induced proarrhythmic risk. *J Chem Inf Model*. 2018;58:867–878. doi: 10.1021/acs.jcim.7b00440
62. Tereshchenko LG, Josephson ME. Frequency content and characteristics of ventricular conduction. *J Electrocardiol*. 2015;48:933–937. doi: 10.1016/j.jelectrocard.2015.08.034
63. Danik S, Cabo C, Chiello C, Kang S, Wit AL, Coromilas J. Correlation of repolarization of ventricular monophasic action potential with ECG in the murine heart. *Am J Physiol Heart Circ Physiol*. 2002;283:H372–H381. doi: 10.1152/ajpheart.01091.2001
64. Qu Z, Xie Y, Garfinkel A, Weiss JN. T-wave alternans and arrhythmogenesis in cardiac diseases. *Front Physiol*. 2010;1:154. doi: 10.3389/fphys.2010.00154
65. Hondeghem LM, Snyders DJ. Class III antiarrhythmic agents have a lot of potential but a long way to go. Reduced effectiveness and dangers of reverse use dependence. *Circulation*. 1990;81:686–690.
66. Hondeghem LM. TRLad: foundation for proarrhythmia (triangulation, reverse use dependence and instability). *Novartis Found Symp*. 2005;266:235–244; discussion 244.
67. Sirenko O, Cromwell EF, Crittenden C, Wignall JA, Wright FA, Rusyn I. Assessment of beating parameters in human induced pluripotent stem cells enables quantitative *in vitro* screening for cardiotoxicity. *Toxicol Appl Pharmacol*. 2013;273:500–507. doi: 10.1016/j.taap.2013.09.017
68. Ben-Ari M, Schick R, Barad L, Novak A, Ben-Ari E, Lorber A, Itskovitz-Eldor J, Rosen MR, Weissman A, Binah O. From beat rate variability in induced pluripotent stem cell-derived pacemaker cells to heart rate variability in human subjects. *Heart Rhythm*. 2014;11:1808–1818. doi: 10.1016/j.hrthm.2014.05.037
69. Mandel Y, Weissman A, Schick R, Barad L, Novak A, Meiry G, Goldberg S, Lorber A, Rosen MR, Itskovitz-Eldor J, Binah O. Human embryonic and induced pluripotent stem cell-derived cardiomyocytes exhibit beat rate variability and power-law behavior. *Circulation*. 2012;125:883–893. doi: 10.1161/CIRCULATIONAHA.111.045146
70. Lakatta EG, Maltsev VA, Vinogradova TM. A coupled SYSTEM of intracellular Ca<sup>2+</sup> clocks and surface membrane voltage clocks controls the time-keeping mechanism of the heart's pacemaker. *Circ Res*. 2010;106:659–673. doi: 10.1161/CIRCRESAHA.109.206078
71. Rubin RJ, Jaeger RJ. Some pharmacologic and toxicologic effects of di-2-ethylhexyl phthalate (DEHP) and other plasticizers. *Environ Health Perspect*. 1973;3:53–59. doi: 10.1289/ehp.730353
72. Aronson CE, Serlick ER, Preti G. Effects of di-2-ethylhexyl phthalate on the isolated perfused rat heart. *Toxicol Appl Pharmacol*. 1978;44:155–169.
73. Jalife J, Zipes DP. *Cardiac Electrophysiology*. 5th ed. Philadelphia, PA: Saunders; 2009:1155.
74. Mariana M, Feiteiro J, Cairrao E. Cardiovascular response of rat aorta to Di-(2-ethylhexyl) phthalate (DEHP) exposure. *Cardiovasc Toxicol*. 2018;18:356–364. doi: 10.1007/s12012-017-9439-6
75. Sheng J, Tran PN, Li Z, Dutta S, Chang K, Colatsky T, Wu WW. Characterization of loperamide-mediated block of hERG channels at physiological temperature and its proarrhythmia propensity. *J Pharmacol Toxicol Methods*. 2017;88(pt 2):109–122. doi: 10.1016/j.vascn.2017.08.006
76. Kirchhof P, Engelen M, Franz MR, Ribbing M, Wasmer K, Breithardt G, Haverkamp W, Eckardt L. Electrophysiological effects of flecainide and sotalol in the human atrium during persistent atrial fibrillation. *Basic Res Cardiol*. 2005;100:112–121. doi: 10.1007/s00395-005-0513-4
77. Tereshchenko LG, Waks JW, Kabir M, Ghafoori E, Shvilkin A, Josephson ME. Analysis of speed, curvature, planarity and frequency characteristics of heart vector movement to evaluate the electrophysiological substrate associated with ventricular tachycardia. *Comput Biol Med*. 2015;65:150–160. doi: 10.1016/j.combiomed.2015.03.001